Bone regeneration and gene expression in bone defects under healthy and osteoporotic bone conditions using two commercially available bone graft substitutes

2015 Biomed. Mater. 10 035003

(http://iopscience.iop.org/1748-605X/10/3/035003)

Biomedical Materials

PAPER

Bone regeneration and gene expression in bone defects under healthy and osteoporotic bone conditions using two commercially available bone graft substitutes

Claire I A van Houdt [1,6], Carla R Tim [1,2,6], Murilo C Crovace [3], Edgar D Zanotto [3], Oscar Peitl [3], Dietmar J O Ulrich [4], John A Jansen [1], Nivaldo A Parizotto [5], Ana C Renno [5] and Jeroen J J P van den Beucken [1]

[1] Department of Biomaterials, Radboudumc, 6500 HB Nijmegen, The Netherlands
[2] Department of Physiotherapy, Federal University of São Carlos (UFSCar), 13565–905 São Carlos, SP-Brazil
[3] Department of Materials Engineering, Federal University of São Carlos (UFSCar), 13565–905 São Carlos, SP-Brazil
[4] Department of Plastic Surgery, Radboudumc, 6500 HB Nijmegen, The Netherlands
[5] Department of Biosciences, Federal University of São Paulo (UNIFESP), 15011-000 Santos, SP-Brazil

E-mail: jeroen.vandenbeucken@radboudumc.nl

RECEIVED
25 November 2014

REVISED
22 February 2015

ACCEPTED FOR PUBLICATION
2 April 2015

PUBLISHED
8 May 2015

Keywords: glass-ceramic, inorganic bovine bone, gene-expression, bone regeneration, osteoporosis

Abstract

Biosilicate® and Bio-Oss® are two commercially available bone substitutes, however, little is known regarding their efficacy in osteoporotic conditions. The purpose of this study was to evaluate the osteogenic properties of both materials, at tissue and molecular level. Thirty-six Wistar rats were submitted to ovariectomy (OVX) for inducing osteoporotic conditions and sham surgery (SHAM) as a control. Bone defects were created in both femurs, which were filled with Biosilicate® or Bio-Oss®, and empty defects were used as control. For the healthy condition both Biosilicate® and Bio-Oss® did not improve bone formation after 4 weeks. Histomorphometric evaluation of osteoporotic bone defects with bone substitutes showed more bone formation, significant for Bio-Oss®. Molecular biological evaluation was performed by gene-expression analysis (Runx-2, ALP, OC, OPG, RANKL). The relative gene expression was increased with Biosilicate® for all genes in OVX rats and for Runx-2, ALP, OC and RANKL in SHAM rats. In contrast, with Bio-Oss®, the relative gene expression of OVX rats was similar for all three groups. For SHAM rats it was increased for Runx-2, ALP, OC and RANKL. Since both materials improved bone regeneration in osteoporotic conditions, our results suggest that bone defects in osteoporotic conditions can be efficiently treated with these two bone substitutes.

1. Introduction

Bone tissue is continuously being turned over and possesses substantial regenerative capacity [1, 2]. Surgical intervention for bone defects can aid bone healing, for which autologous bone graft (i.e. transplantation) remains the golden standard [3, 4]. However, drawbacks for this procedure are increased donor site morbidity, the limited amount and quality of autologous bone available, and a prolonged surgical time [3–7]. To overcome these disadvantages, research has focused on the development of either organic or synthetic bone substitutes to replace the need for autologous bone grafting [3, 6].

Especially in compromised conditions such as infections, malignancy or increased age of the patient, bone healing is impaired and requires surgical intervention. Osteoporosis is such a compromised condition that can interfere with bone healing and is affecting a rapidly increasing number of people. In the United States, osteoporosis affects ~10 million individuals aged >50 years, with an additional 34 million people considered to be at risk [8]. Worldwide, 9 million new osteoporosis-related fractures are estimated to occur each year [9], two million of which occur in the United States alone [10]. As osteoporosis is associated with an immense socioeconomic significance, it has been recognized as a major public health problem [11]. Osteoporosis is a complex disease characterized by a decrease of bone mass and associated with (i) a decreased proliferative activity of osteoblast progenitor cells and gene expression [12], (ii) an impaired osteoblast function [13], (iii) a diminished osteoblast response to signalling [14], and (iv) an imbalance between bone formation and resorption [15].

[6] Equally contributed.

To summarise, compromised patients such as those suffering from osteoporosis could benefit greatly from the use of bone graft substitutes with enhanced osteogenic activity. From a bone substitute material perspective, interaction of the material with bone tissue should favour bone regenerative processes for compromised patients [16, 17]. Several bone substitute materials are commercially available for clinical applications nowadays. Worldwide, research is performed to enhance the properties of bone substitute materials and hence their biological performance [18]. Bio-Oss®, made from the mineral part of bovine bone, is a well-established bone substitute material and represents the major clinically-used product for dental bone regeneration [19]. It has been documented that Bio-Oss® promotes osteogenesis *in vitro* [20, 21]. During the production process, the organic parts are removed from the bovine bone and the remaining calcium-containing bone structures are processed to slowly degradable granules [22]. Furthermore, many approaches have explored the potential of materials with a high bioactivity rate, such as bioactive glasses (BGs) and glass-ceramics (BGCs), for bone regenerative applications [23–25]. BGCs, including Biosilicate®, are synthetic silica-based bioactive materials, with the unique ability to directly bond to bone tissue, making these materials appealing for bone regeneration [25–28]. Research results indicate that upon degradation of such a silica-based material, silicon, calcium (Ca^{2+}), phosphate (PO_4^{2-}), and sodium (Na^+) ions are released in the physiological environment and suggest that a combination of these ions stimulates cells to form new bone tissue [29]. Biosilicate® is a novel bone substitute glass-ceramic (crystalline) material and there are various studies underlining its suitability for bone replacement and potential to facilitate new bone formation [30–32]. For example, Granito *et al* [30, 31] investigated the effects of Biosilicate® with 2 different particle size distributions (180–212 and 300–355 μm) on bone healing in a tibial bone defect model in rats. At 20 d after implantation they observed that bone defects filled with particles of Biosilicate® (180–212 μm in diameter) showed a higher amount of newly formed bone in the area of the callus and improved biomechanical properties compared to (empty) control animals and to animals treated with original 45S5 Bioglass®. Furthermore, molecular biology studies have shown that a solution containing Ca, P and Si ions stimulates gene expression (of amongst other growth-related genes, cell adhesion receptor genes, and matrix metalloproteinase genes) in osteoblasts [33].

Pre-clinical testing of newly developed bone substitute materials is generally done using healthy animals. In view of the heterogeneity of patients that require bone regenerative treatment, these studies do not provide information on bone substitute material performance in compromised bone conditions, such as in osteoporotic bone. In view of the lack of knowledge on the performance of clinically available bone substitute materials in different bone conditions, we aimed at comparatively using a rat femoral condyle bone defect model for rats that had either or not undergone ovariectomy to induce an osteoporotic bone condition [34]. Within the created bone defects in healthy and osteoporotic bone, we used Biosilicate® or Bio-Oss® and evaluated the biological performance of these bone substitute materials as well as their effects on *in vivo* gene expression. Additionally, we evaluated the *in vitro* cellular response to these bone substitute materials.

2. Materials and methods

2.1. Materials

Biosilicate® (fully crystallized bioactive glass ceramic of the quaternary Na_2O–CaO–SiO_2–P_2O_5 system, containing weight percentages of respectively 23.75, 23.75, 48.5 and 4%) was provided by Vitreous Materials Laboratory, Department of Materials Engineering, Federal University of São Carlos (São Carlos, São Paulo, Brazil) [35]. Bio-Oss® was purchased from Geistlich Pharma AG (Wolhusen, Switzerland). The materials used were in the form of dense particles (size: 0.25–1 mm).

2.2. In vitro *biological response to Biosilicate® and Bio-Oss®*

2.2.1. Cell culture

Cryo-preserved rat bone marrow stromal cells (BMSC) were employed in this study. BMSCs were grown in minimum essential medium (MEM-α; Gibco BRL, Life Technologies, Breda, the Netherlands) supplemented with 10% foetal bovine serum (FBS; Gibco), and penicillin/streptomycin (100 units ml^{-1}; Gibco). All tissue culture procedures were performed under strict aseptic conditions in a biological safety cabinet. BMSCs were grown in sterile, vented, tissue culture flasks (75 cm^2; Greiner Bio-one, Utrecht, The Netherlands) in a humidified incubator at 37 °C in 5% carbon dioxide (CO_2), 95% air. The cells were expanded for five passages using standard tissue culture techniques.

2.2.2. Pre-incubation of Biosilicate® particles and cell seeding

Prior to cell seeding, Biosilicate® (0.025 grams) was placed in 24-well ThinCert™ cell culture inserts (Greiner Bio-one) and incubated in tissue culture growth medium supplemented with 25 mM HEPES (Sigma-Aldrich, Zwijndrecht, The Netherlands) and 10% FBS (Gibco) at 37 °C, 5% CO_2 for at least 48 h, in order to decrease the pH of the medium to allow for cell culture. After this period, the medium was discarded. This pre-incubation of Biosilicate® is needed, because the ion exchange reaction which are known to occur at the surface of bioactive glasses in physiological environment can lead to an increase of media pH with cytotoxic effects [36]. Bio-Oss® particles (0.025 grams) were also placed in 24-well ThinCert™ cell culture inserts (Greiner Bio-one), but

without the need of pre-incubation. Subsequently, BMSCs were seeded in direct contact with the particles at a density of 20 000 cells/insert. Cell culture medium was changed every 2–3 d, and the cells were cultured for up to 28 d.

2.2.3. Determination of cell metabolic activity

Cell metabolic activity was evaluated using AlamarBlue® (Invitrogen, Life Technologies, Breda, The Netherlands) according to the manufacturer's instructions. Briefly, AlamarBlue® (1 ml) was added directly to BMSCs in cell culture media ($n = 8$) and the plate was incubated for 4 h at 37 °C in a cell culture incubator. Subsequently, 200 μl of each sample was transferred to a 96 well plate (in duplicates). Finally, the plate was read in a spectrophotometer (Bio-Tek Instruments, Winooski, USA) at 570 nm.

2.2.4. Cell proliferation

Cell proliferation was determined by quantifying the amount of DNA (QuantiFluor® dsDNA quantitation kit; Promega, Leiden, The Netherlands). After 7, 14 and 28 d of culture, BMSCs were washed with PBS ($n = 8$), homogenized in ultrapure water (1 ml), frozen, and thawed twice before analysis. Then, the DNA sample (100 μl) or standard was incubated with working solution (100 μl) in the dark for 10 min. Finally, the samples were read in a spectrophotometer (Bio-Tek Instruments) at 530 nm.

2.2.5. ALP activity

The specific activity of alkaline phosphatase (ALP) was assayed by the use of an ALP activity assay (Sigma). Briefly, 80 μl sample ($n = 8$) or standard (serial dilutions of 4-nitrophenol at the concentrations of 0–25 nM) and 20 μl buffer solution (0.5 M 2-amino-2-methyl-1-propanol) were added into a 96-well plate. Then, a substrate solution (p-nitrophenyl phosphate; 100 μl) was added to all the wells and subsequently the mixture was incubated at 37 °C for 1 h. The reaction was stopped by adding of 0.3 M NaOH (100 μl), and the ALP activity was measured in a spectrophotometer (Bio-Tek Instruments) at 405 nm with subsequent normalization for DNA content.

2.2.6. Calcium content

After 7, 14, and 28 d of culture, the amount of deposited calcium by BMSCs ($n = 8$) was quantified using the ortho-cresolphthalein complexone method (Sigma). Briefly, cell layers were washed twice with PBS, and then incubated in 0.5 N acetic acid (1 ml) on a shaking platform overnight. For analyses, a sample (10 μl) or standard was incubated with work reagent (300 μl) in a 96-well plate at room temperature for 10 min. The standards (0–100 mg ml^{-1}) were generated by serial dilutions of a $CaCl_2$ stock solution. Finally, the plate was read in a spectrophotometer reader (Bio-Tek Instruments) at 570 nm. Negative control reactions with particles (Biosilicate® and Bio-Oss®) without cells were also included in each assay and it was used to normalize deposition calcium data.

2.2.7. Scanning electron microscopy (SEM)

On days 7, 14 and 28 post-seeding, biomaterial particles with attached cells were washed twice with PBS and fixed for 10 min using glutaraldehyde (2% in 0.1 M cacodylate buffer). Subsequently, the samples were washed with 0.1 M cacodylate buffer (pH 7.4) and dehydrated in graded series of ethanol. Finally, samples were dried with tetramethylsilane (Sigma), sputter coated with gold and examined using a scanning electron microscope (JEOL 6310, Nieuw-Vennep, The Netherlands).

2.2.8. RNA isolation

Total RNA was isolated from the cells using TRIzol reagent (Invitrogen) ($n = 5$ per group) according to the manufacturer's instructions. In brief, after removing the culture medium, TRIzol reagent (1 ml) was added to each well. The cell extract was mixed vigorously with chloroform (0.2 ml) and centrifuged at 12 000 g for 15 min at 4 °C. The aqueous phase of the sample was collected and mixed with 100% isopropanol (0.5 ml). After incubation at room temperature for 10 min, the extract was centrifuged and then washed with 75% ethanol. Successively, the RNA pellet was dissolved in RNase-free water and concentration and purity were determined using the NanoDrop (ND-2000; Thermo Scientific, Waltham, MA USA). RNA samples with an A260/A280 ratio <1.8 were excluded.

2.2.9. Real-time PCR

Total RNA (1 μg) was applied as template for cDNA synthesis using the iScript cDNA synthesis kit (Bio-Rad, Veenendaal, the Netherlands) following the manufacturer's instructions. The cDNA samples were subjected to quantitative real time polymerase chain reaction (qRT-PCR) using a BIORAD CFX96 real-time system.

Oligonucleotide primers were designed for RPS18 (NM_181374.2), Runx-2 (NM_053470.2), alkaline phosphatase (ALP) (J03572.1), Osteocalcin (OC) (NM_013414.1) (table 1) using Primer Express Software 2.0 (Applied Biosystems, Foster City, USA). All real-time primers were initially tested against standards and a standard curve was generated.

The optimized PCR conditions were: initial denaturation at 94 °C for 10 min, followed by 40 cycles consisting of denaturation at 94 °C for 15 s, annealing at 60 °C for 1 min, and extension at 72 °C for 45 s, with a final extension step at 72 °C for 2 min. Negative control reactions with no template (deionised water) were also included in each run. For each gene, all samples were amplified simultaneously in duplicate in one assay run. Analysis of relative gene expression was performed using the $2^{-\Delta\Delta CT}$ method. RPS18 was used as a housekeeping gene to normalize expression data.

Table 1. Primers and the expected PCR product size at indicated annealing temperatures for each gene analyzed. RPS18: ribosomal protein S18; Runx-2: runt-related transcription factor 2; ALP: alkaline phosphatase; OC: Osteocalcin; RANKL receptor activator of nuclear factor kappa-B ligand; OPG: Osteoprotegerin.

Gene	Forward primer	Reverse primer	Annealing temperature
RPS18	GTGATCCCCGAGAAGTTC	AATGGCAGTGATAGCGAA	60 °C
Runx-2	TTATGTGTGCCTCCAACCTGTGT	GGTTTCTTTCCCCCTCAATTTGT	60 °C
ALP	AACTACATCCCCCACGTCATG	CCCAGGCACAGTGGTCAAG	60 °C
OC	ACGAGCTAGCGGACCACATT	CCCTAAACGGTGGTGCCATA	60 °C
RANKL	CCGTTTGCTCACCTCACCAT	TGGTACCAAGAGGACAGACTGACTT	60 °C
OPG	GATATTGCCCCCAACGTTCA	AGGGCGCATAGTCAGTAGACACT	60 °C

2.3. Animal experiment

2.3.1. Animal model and validation

For this experiment, 36 mature female Wistar rats were used (weight ~250 g; Charles River Nederland B.V., Leiden, The Netherlands). A 1 week acclimatization period was maintained in standard housing (i.e. 2 rats per box). All rats received two surgical procedures during the course of the experiment: the first surgery was a bilateral ovariectomy (OVX; 19 rats) to induce an osteoporotic bone condition or a sham operation (SHAM; 17 rats) for a healthy bone condition; in the second surgery, bone defects were created in both femoral condyles (bilateral) of all animals, which were left empty as control or filled with Biosilicate® or Bio-Oss®. Access to food and bottled water was maintained *ad libitum*. All experiments were in accordance with institutional, national and international guidelines for animal care and the Dutch law concerning animal welfare. The studies were reviewed and approved in advance by the Experimental Animal Committee of the Radboud University (RUDEC 2013–187).

2.3.1.1. Surgery to induce osteoporotic condition

Nineteen animals received an ovariectomy (OVX) through two separate incisions in the lateral abdominal wall [34]. The remaining seventeen rats received a sham surgery (SHAM) using an identical surgical approach as for the other animals without removal of the ovaries. Pre-operatively, pain medication was provided 15 min before surgery by injecting Carprofen (5 mg kg^{-1}; Rimadyl®, Pfizer Animal Health, New York, USA). Anaesthesia was induced and maintained by isoflurane inhalation (2–5%; Rhodia Organique Fine Limited). The back area was shaved and disinfected with a povidone iodine solution. The animal was placed on an electric heating mat in prone position to prevent hypothermia. A dorsal midline incision (~2 cm) caudal to the posterior border of the ribs was created to enter the abdominal cavity. The ovary was located in a fat pad and gently pulled outside the abdominal cavity. A single ligature was placed around the fallopian tube using a surgical polyester suture (Terylene® 2.0 undyed, Serag-Wiessner GmbH and Co, Naila, Germany). The ovary was removed by cutting above the ligated area and after haemostasis the tuba was returned into the abdomen. The abdominal muscles were closed with continuous absorbable sutures (Vicryl® 4.0, Ethicon, Amersfoort, The Netherlands) after which the skin was sutured with multiple single absorbable sutures (Vicryl® 4.0, Ethicon). The procedure was repeated for the contro-lateral ovary using the same incision design. Postoperative pain medication for a minimum of 2 d was provided by injection of Carprofen every 24 h and Buprenorfine (0.02 mg kg^{-1}; Temgesic®, Reckitt Benckiser Health Care Limited) every 12 h. To ensure progression toward an osteoporotic bone condition, the OVX group received a low calcium diet of pellets containing 0.01% calcium and 0.77% phosphorous (Ssniff Spezialdiäten GmbH, Soest, Germany) for six weeks, whereas the SHAM group received no dietary restrictions.

2.3.1.2. Surgery for femoral bone defect and material implantation

Six weeks after OVX or SHAM surgery, a bone defect was created in both femoral condyles of each animal. Anaesthesia and pain medication were administered as described for the first operation. Both hind limbs of the rats were shaved and disinfected with povidone iodine. The rats were immobilized in supine position on a heating mat. A longitudinal incision through skin and muscle was made on the medial surface of the knee in flexed position. After exposure of the medial side of the distal femoral condyle the knee capsule was incised. By extension of the knee, luxation of the patella laterally was possible. When a clear view of the femoral side of the knee joint was established, a defect longitudinal to the length of the femur (Ø 2.5 mm by 6 mm in depth) was created. To create the defect, a dental drill (Elcomed 9927 SPS; W and H Dentalwerk Burmoos GmbH, Burmoos, Austria) with a series of increasing bur diameters were used at a speed of maximum 5000 rpm and a constant cooling using saline. The defect was either left empty as control or filled with Biosilicate® or Bio-Oss®. The muscular layer and skin were closed with single resorbable sutures (Vicryl® 4.0 Ethicon). After implant surgery, both experimental groups (SHAM and OVX) had free access to normal pellet food and water. The animals were housed per pair under the same conditions. In the initial postoperative period, the intake of water and food was monitored as well as the weight of the animals. In addition, the animals were observed for signs of pain, infection and proper activity and weighed again postoperatively once a week to

identify significant weight loss (>20%) compared to preoperative body weight of each rat.

2.3.1.3. Validation of osteoporotic condition by ELISA for serum TRAP analysis

The osteoporotic condition by OVX was evaluated by a serum analysis for TRAP enzyme activity performed with the RatTRAP™ Assay kit (Immunodiagnostic Systems GmbH, Frankfurt am Main) at the end of the experiment, 4 weeks after implantation surgery.

2.3.1.4. Retrieval of specimens

The femurs were retrieved 4 weeks after implantation surgery. The femurs used for gene expression of both osteoporotic ($n \geq 6$) and healthy conditions ($n \geq 5$) were placed on ice for transport and immediately processed for RNA isolation. The femurs needed for histology of both osteoporotic ($n \geq 5$) and healthy conditions ($n \geq 4$) were immediately fixed in 10% formaldehyde for 24 h, and then dehydrated in 70% ethanol. After dehydration, one femur of each group was scanned by micro-CT, then all femurs for histology were embedded in polymethylmethacrylate (pMMA), prepared by mixing methylmethacrylate (600 ml; Acros Organics BVBA, Geel, Belgium) with dibutyl phthalate (60 ml; Merck KGaA, Darmstadt, Germany) and Perkadox 16 (1.25 g; AkzoNobel, Amersfoort, The Netherlands).

2.3.2. Micro-CT

A desktop micro-CT system (Skyscan-1072, TomoNT version 3 N.5, Skyscan®, Kontich, Belgium) was used for 3D imaging. The specimens were placed with the long axis of the implant perpendicular to the scanning beam, after which a high resolution scan was performed. 3D reconstruction and imaging processing was performed using NRecon V1.4 and CTvox v2.7 (Skyscan®), respectively.

2.3.3. Histology

After polymerization, thin sections (~10–15 μm) in perpendicular to the longitudinal direction, were prepared using a diamond blade microtome (Leica® Microsystems SP 1600, Nussloch, Germany). A minimum of three sections of each specimen were stained with methylene blue and basic fuchsine and examined using light microscopy (Leica® Microsystems AG, Wetzlar, Germany).

2.3.4. Histomorphometry

Using an imaging microscope (Axio Imager Microscope Z1, Carl Zeiss Micro Imaging GmbH, Göttingen, Germany), the pMMA-embedded histological sections were digitalized (5 × magnification). Quantitative analysis of the digitalized images was performed using ImageJ software (Java® ImageJ 1.47, Image processing and analysis in Java). Within a circular region of interest (ROI) with an equal diameter (2.5 mm) to the created bone defects, the amount of newly formed bone was determined. Vital bone could be distinguished by the pink colour and distinctive cell morphology including a nucleus, allowing to be easily discerned from other tissues as wells as from Biosilicate® and Bio-Oss® particles. The maturity of bone was differentiated by morphology, as mature trabecular bone is formed in lamellae, whereas newly formed bone has a more woven structure. Detection of different cell types could be performed as osteocytes are trapped within the lacunae of bone, osteoblasts are arranged in rows with basophilic eccentric nuclei and osteoclasts are relatively larger and multinucleated cells.

2.3.5. In vivo *gene-expression*

For RNA isolation, the femurs were dissected and the bone defect area was trephined (inner diameter of 2.5 mm) using drilling equipment (Weiss Machine WMD20LV, Jiangsu Province, China). The retrieved tissues were placed in sterilized microtubes (1.5 ml) and frozen at −80 °C until analysis. To facilitate processing of multiple samples, the Bullet Blender (Next Advance, New York, USA) was used with centrifuge technology that homogenizes tissue by bead disruption of the tissue. The bone sample was added to a pre-chilled microtube containing the beads recommended by the manufacturer for RNA isolation (~50 μl stainless steel blend, 6 × 3.2 mm stainless steel) followed by the addition of TRIzol reagent (600 μl; Invitrogen). The bone was homogenized in the Bullet Blender (Next Advance) centrifuge (kept in a cold room at 4 °C) for 5 min, then the solubilised bone extract was isolated by centrifugation for 15 s at 8.600 rpm at room temperature and the solution was transferred to a new microtube. Then, the RNA protocol was performed using TRIzol reagent according to the manufacturer's instructions.

The cDNA and real time PCR procedures were performed as described above for *in vitro* experimental work. In addition to the primers used for *in vitro* experimental work, primers for osteoprotegerin (OPG; NM_012870.2) and RANKL (AF187319.1; table 1) were used.

2.4. Statistical analysis

Data are presented as mean with SDs. Statistical analysis of quantitative data was performed using one-way analysis of variance (ANOVA) with a Tukey post-hoc test. GraphPad Software (PRISM; La Jolla CA, USA) was used to carry out the statistics analysis. For a comparison between both conditions and for the analysis of the serum TRAP enzyme, a one-tailed student t-test was used. Values of $p < 0.05$ were considered statistically significant.

3. Results

3.1. In vitro *biological response of Biosilicate® and Bio-Oss®*

The metabolic activity of rat bone marrow stromal cells (BMSCs) seeded on the materials and control samples

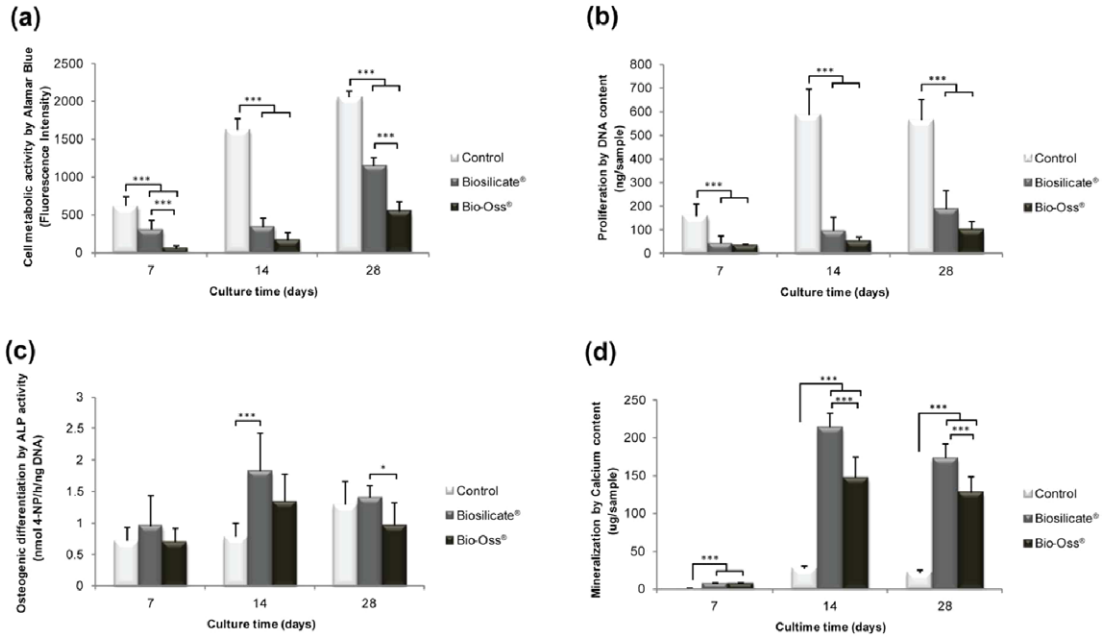

Figure 1. (a)–(d) *In vitro* biological response analysis (mean ±SD; $n = 8$). (a) Cell metabolic activity. (b) DNA content (cell proliferation). (c) ALP-activity (as a marker of early differentiation). (d) Calcium content (as a marker of late differentiation); $^{*}p < 0.05$, $^{***}p < 0.001$.

showed a temporal evolution during the culture period. On days 7, 14 and 28, the cell metabolic activity was significantly higher for controls (on tissue culture plastic) compared to either Biosilicate® or Bio-Oss® ($p < 0.001$; figure 1(a)). Furthermore, the cell metabolic activity of rat BMSCs on Biosilicate® was significantly increased compared to Bio-Oss® on both day 7 and 28 ($p < 0.001$; figure 1(a)). For cell proliferation (figure 1(b)), controls showed significantly increased DNA-content values ($p < 0.001$) compared to both Biosilicate® and Bio-Oss® at each time point. As a marker for early osteogenic differentiation, ALP-activity showed a peak for both Biosilicate® and Bio-Oss® on day 14 (figure 1(c)), whereas a continuous increase in ALP-activity was observed for controls. BMSCs cultured on Biosilicate® showed a significantly increased ALP-activity compared to controls at day 14 ($p < 0.001$) and compared to Bio-Oss® at 28 d ($p < 0.05$). As a marker for late osteogenic differentiation, extracellular calcium deposition (figure 1(d)) on both Biosilicate® and Bio-Oss® was significantly higher ($p < 0.001$) compared to controls at all time points. Further, cells in contact with Biosilicate® deposited more calcium by day 14 and 28 compared to Bio-Oss® ($p < 0.001$). Morphologically, SEM analysis showed that rat BMSCs were successfully grown on Biosilicate® and Bio-Oss® particles at all time points (data not shown).

3.1.1. *Real time PCR*

Figures 2 (a)–(b) represents the gene expression data of rat BMSCs cultured on Biosilicate®, Bio-Oss®, and tissue culture plastic controls after culture for 7, 14 and 28 d. Significantly increased Runx-2 expression (figure 2(a); $p < 0.05$) was observed for rat BMSCs cultured on Biosilicate® compared to controls after 14 d. For rat BMSCs cultured on Biosilicate® and Bio-Oss®, the expression of OC (figure 2(b)) was significantly increased compared to controls after 7 and 14 d ($p < 0.05$) and 28 d ($p < 0.05$), respectively. Similar ALP gene expression levels were observed for all experimental groups (figure 2(c)).

3.2. Animal experiment

3.2.1. *Animal model and validation*

Validation of the osteoporotic condition in this study was performed by a serum TRAP ELISA analysis. Our data showed that rats with osteoporotic bone condition had significantly decreased serum TRAP enzyme activity ($p < 0.0001$) compared to healthy rats (figure 3). Clinical observations after OVX and bone defect surgery showed that SHAM surgery led to euthanisation of one rat, due to >20% weight loss in the first week postoperatively related to intestinal problems. Upon implantation surgery, two rats (one OVX, one SHAM) were euthanized due to fracture of the femur during the drilling of the bone defect. All remaining rats recovered without clinical signs of complications and remained healthy during course of the experiment.

3.2.2. *Micro-CT*

An overview of 3D reconstructed bone defects from *ex vivo* micro-CT is presented in figure 4, showing sagittal, frontal and transverse planes through the defect area for each experimental group after 4 weeks of implantation. The images provide information on the amount and space between trabecular bone as well as the distribution of and space between the particles.

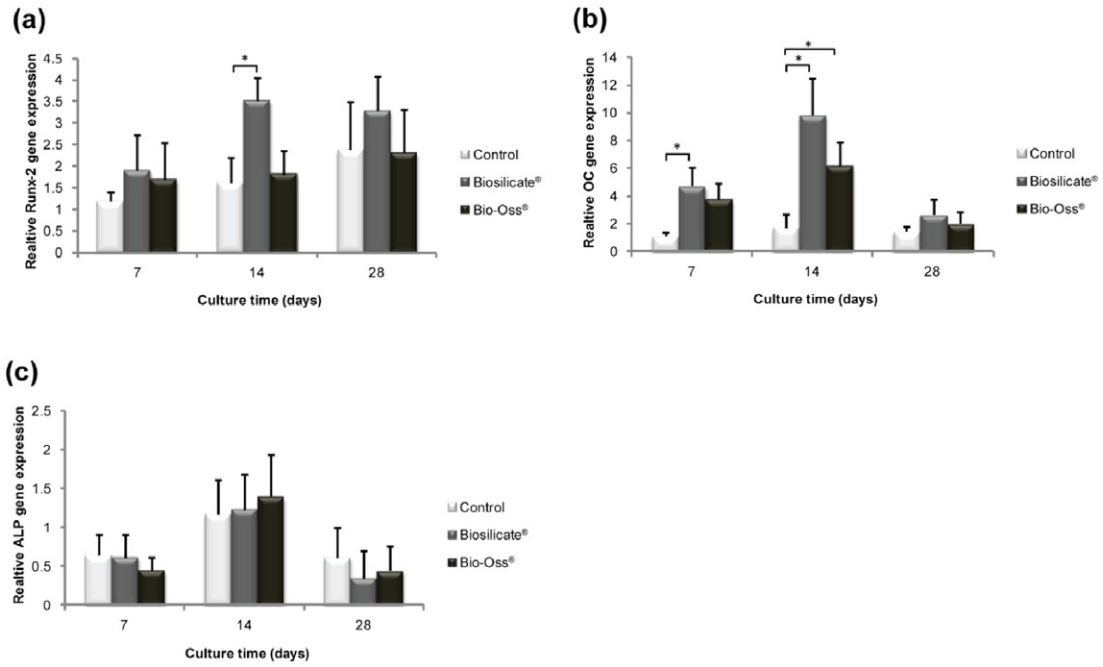

Figure 2. (a)–(c) *In vitro* results of the relative quantification of gene expression levels from BMSCs ($n = 8$), mean ±SD. (a) Runx-2 gene-expression. (b) OC gene-expression. (c) ALP gene-expression; * $p < 0.05$.

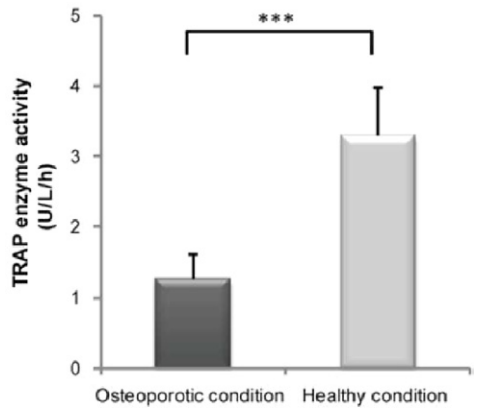

Figure 3. Serum TRAP enzyme activity (mean ±SD) in rats with osteoporotic and healthy bone condition ($n = 5$); *** $p < 0.001$.

3.2.3. *Histology*

Representative histological images at 4 weeks after implantation for each of the experimental groups are presented in figure 5. Histological differences were observed between osteoporotic and healthy bone conditions regarding the amount and spacing of the trabecular bone outside the ROI. The space between the trabeculae was filled with bone marrow. The empty defects clearly showed that bone regeneration starts at the edges of the defect, growing inwards. The circumference of Biosilicate® and Bio-Oss® particles was mostly covered with newly formed bone, all the way to the centre of the defect. This shows the osteoconductive properties of both Biosilicate® and Bio-Oss®, as this was never reached by the empty defects in the osteoporotic conditions. Our histological images clearly showed a gel-like layer to be present on the Biosilicate® particles implanted in both conditions (black arrows in figure 5).

3.2.4. *Histomorphometry*

Quantitative histomorphometry showed material new bone formation around the Biosilicate® and Bio-Oss® particles with remnant amounts for both osteoporotic and healthy conditions compared to empty controls (table 2 and figures 6 (a)–(c)). Osteoporotic conditions lead to bone formation (means with SDs) of respectively 5 ± 8%, 11 ± 4% and 15 ± 5% for the empty control, Biosilicate® and Bio-Oss®, compared to respectively 20 ± 9%, 14 ± 5% and 16 ± 4% in healthy conditions. For the empty defects, a significant difference ($p < 0.05$) for bone formation was seen between the osteoporotic and healthy conditions, again underlining the systemic effect of OVX surgery.

3.2.5. *Real time PCR*

To progress in the understanding of the mechanisms by which the process of bone healing is influenced in the presence of Biosilicate® and Bio-Oss®, an evaluation of gene expression for bone formation-related genes was performed. Expressions of the selected osteogenic genes in osteoporotic and healthy conditions are shown in figures 7 (a)–(e), measured at 4 weeks after implantation of Biosilicate® and Bio-Oss®. The relative gene expression showed that in osteoporotic conditions, Biosilicate® increases Runx-2, ALP, OC, OPG and RANKL expression. Bio-Oss® did not up-regulate either of the selected genes in osteoporotic conditions compared to controls. In healthy conditions, Biosilicate® demonstrated an up-regulation of Runx-2, ALP, OC and RANKL, while Bio-Oss® up-regulated

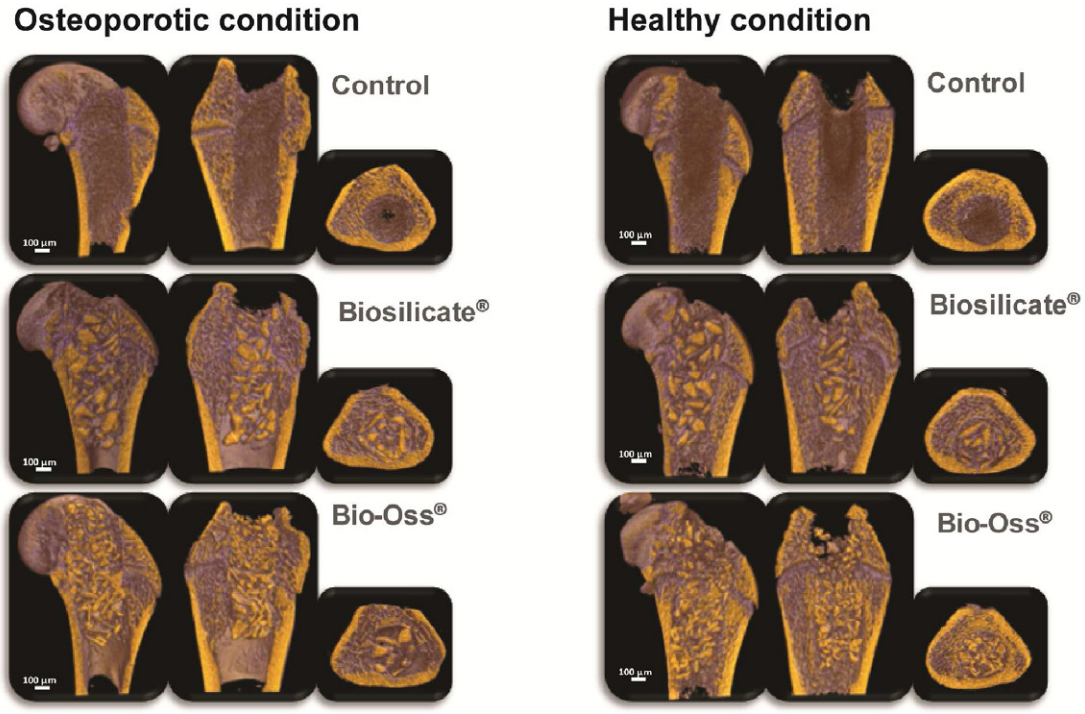

Figure 4. Representative 3D-reconstructions of the defect area obtained via *ex vivo* micro-CT.

only Runx-2, ALP and RANKL gene expression. Between the materials significantly more expression of Runx-2 and RANKL was seen for Biosilicate® in osteoporotic conditions and of OC and RANKL in healthy conditions.

4. Discussion

The biological performance as well as the effects on *in vivo* gene expression of Biosilicate® and Bio-Oss® were comparatively examined using a rat femoral condyle bone defect model for rats that had either or not undergone ovariectomy to induce an osteoporotic bone condition [34]. Additionally, we evaluated the *in vitro* cellular response to these bone substitute materials.

Our *in vitro* experiments showed BMSCs can proliferate on tissue culture plastic. More importantly however, the addition of Biosilicate® and Bio-Oss® stimulated osteogenic differentiation compared to controls. These data corroborates the results of Ozawa *et al* [37] showing stimulated osteogenic differentiation of rat BMSCs upon culturing rat bone marrow cells on hydroxyapatite (HA). When cultured on Biosilicate®, there was significantly more mineralization compared to Bio-Oss®, suggesting Biosilicate® to have more osteogenic potential *in vitro*. These findings are supported by the study by Renno *et al* [38], who using *in vitro* experiments observed that osteogenic cells were successfully grown on Biosilicate® scaffolds. Moreover, the study by Herten *et al* [39] showed, when seeding cells on Bio-Oss® granules, a smaller number of viable osteoblasts were detectable on the granules compared to other bone graft substitutes.

A significant up-regulation of Runx-2 was induced *in vitro* by Biosilicate® after 14 d. Although in our study Bio-Oss® did not induce an up-regulation of Runx-2, Sollazzo *et al* [40] showed that cells cultured on Bio-Oss® for 7 d increase the osteoblast transcriptional factor Runx-2 together with other bone-related genes, i.e. SPP1 and FOSL1. Both Biosilicate® and Bio-Oss® increased the expression of OC, which corroborates with our biochemical results showing an increased mineralization compared to controls.

For evaluation of the effect of osteoporosis on bone healing in animal studies, several animal models have been utilized [41, 42]. The ovariectomised rat model is a well-established small animal model for local osteoporosis [41–44]. Ovariectomy leads to estrogen deficiency and hence mimics post-menopausal osteoporosis. Since dietary factors play an important role in the multi-factorial nature of bone loss, an additional low calcium diet can further establish the osteoporotic effect [34, 45]. Previous studies based on *in vivo* micro-CT analysis demonstrated significant effects on bone density and morphological characteristics within the femoral condyles of rats at six weeks after ovariectomy and a low calcium diet [34].

Our serum analysis results for TRAP enzyme activity are in agreement with the study of Rissannen *et al* [46], who also showed significantly lower serum TRAP-activity in the OVX operated rats. Serum TRAP is a marker for the bone homeostasis, providing information about bone resorption, as the TRAP enzyme activity is derived exclusively from osteoclasts [46]. The amount of active osteoclasts on a systemic level is indicated by serum TRAP-activity. Initially, serum TRAP-activity is expected to rise after OVX surgery,

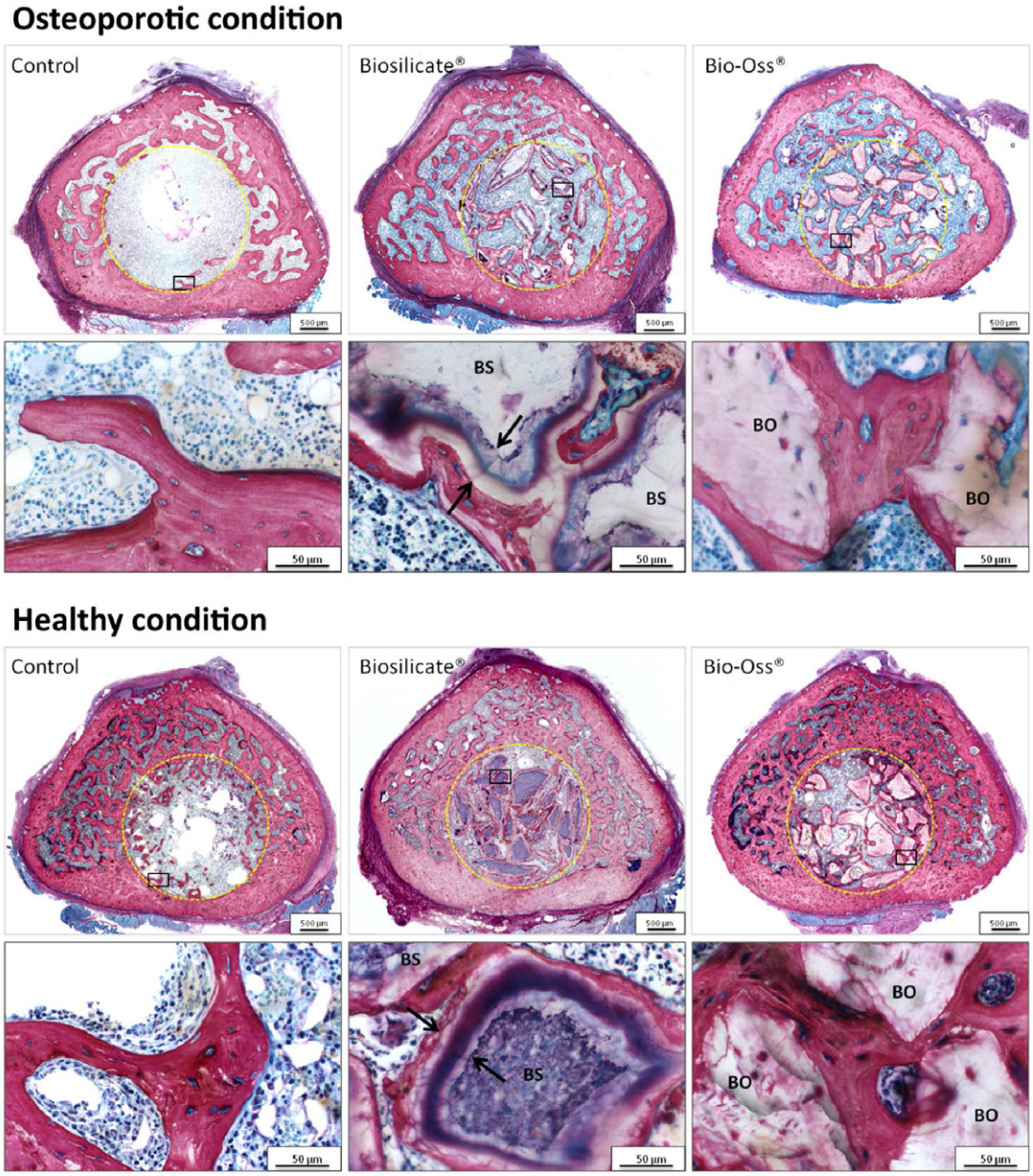

Figure 5. Images of histological slides of osteoporotic and healthy conditions with detailed images (black box), yellow circle = ROI (equal to defect of 2.5 mm), BS = Biosilicate® particles, BO = Bio-Oss® particles; arrows indicate the Biosilicate® silica-layer.

because bone resorption is increased. However, due to the resorption the absolute number of osteoclasts is significantly decreased, consequently lowering TRAP-activity in serum [46]. The additional value of serum TRAP analysis has over *in vivo* micro-CT, is to confirm that the osteoporotic condition is still effective locally at defect site (created 6 weeks post-ovariectomy) and even systemically after an additional implantation period of 4 weeks.

Images from *ex vivo* micro-CT 3D reconstructions provide information on the amount and space between trabecular bone as well as the distribution of and space between the particles. An osteoporotic condition had apparently less trabecular bone compared to healthy condition and the trabecular spacing appeared larger. Filling of the defects with Biosilicate® and Bio-Oss® showed different packing, with a loose filling for Biosilicate® and more compact filling for Bio-Oss®. Despite similar granule sizes and amounts, granule size distribution differences, apparently led to packing differences in the defects [47]. Also surface area can vary

Table 2. Percentages (mean ±SD) of new bone formation within the ROI of osteoporotic ($n \geq 5$) and healthy conditions ($n \geq 4$); significant difference compared to the osteoporotic control group.

	Control		Biosilicate®		Bio-Oss®	
	Mean	SD	Mean	SD	Mean	SD
Osteoporotic condition	5	± 8	11	± 4	15[a]	± 5
Healthy condition	20[b]	± 9	14	± 5	16	± 4

[a] $p < 0.05$.
[b] $p < 0.01$.

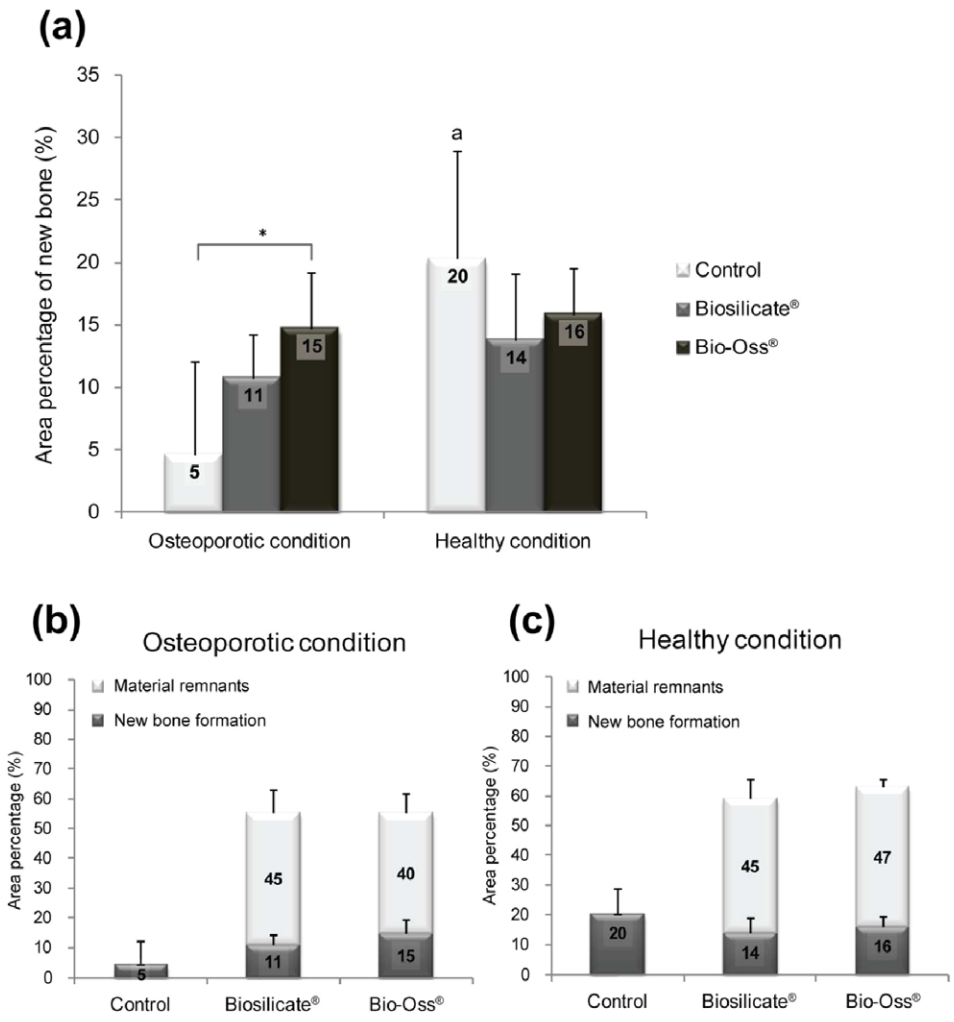

Figure 6. (a) Percentage (mean ±SD) of new bone formation and material remnants within ROI of osteoporotic ($n \geq 5$) and healthy conditions ($n \geq 6$). (b) New bone formation with addition of material remnants within ROI of osteoporotic and (c) healthy conditions; * $p < 0.05$, [a] $p < 0.01$.

due to these granule size distribution differences. Both materials were used in the form available for clinical application for translational power.

The histological images clearly showed a gel-like layer on the Biosilicate® particles implanted in both conditions. It is well known that bioactive glasses (BG) undergo a series of reactions following implantation [47]. Release of ions (Si, Na, Ca and P) occurs immediately upon contact of BG with fluids, resulting in an increased pH [23, 47, 48]. Dissolution and repolymerisation of silica occur to form a silica gel on the surface. Amorphous calcium phosphate nucleates and grows onto and into the SiO_2-rich layer. With time, the CaO–P_2O_5 mineral incorporates carbonate and hydroxyl species from the ambient fluid, and hydroxycarbonate apatite (HCA) crystallizes. This layer is a necessary requirement for bone bonding to occur [17].

In the osteoporotic conditions, Bio-Oss® significantly improved bone formation. Several studies on Bio-Oss® already described the excellent *in vivo* performance of this bone graft material [49, 50]. The *in vivo* results of this study demonstrate that local osteogenic effects are significantly induced by Bio-Oss® compared to empty defects. The surfaces of the Bio-Oss® granules provide a source of calcium ions, possibly facilitating bone formation around the granules [51].

For the healthy condition, both Biosilicate® and Bio-Oss® did not improve bone formation, showing the limits of using bone substitute materials in non-critical sized defect in healthy conditions. Because trabecular bone is spaced, to calculate the maximal amount of bone normally present in that area of the femur, a reference measurement could be taken from undamaged bone. This was performed earlier in the study of van de Watering *et al* [52], where a femoral condyle defect was used filled with injectable calcium phosphate cement. Bone formation was calculated and comparatively evaluated to the contra lateral undamaged bone. These bone volumes were 43 ± 3% and 32 ± 2% at 4 weeks after ovariectomy respectively for healthy and osteoporotic bone conditions (unpublished data by van de Watering *et al* 2013), using a similar strain of rats and dietary protocol as in our study. Our results show that bone formation has not reached the optimal amount after 4 weeks, because even for the empty bone defects a lower amount of bone area was detected. To understand

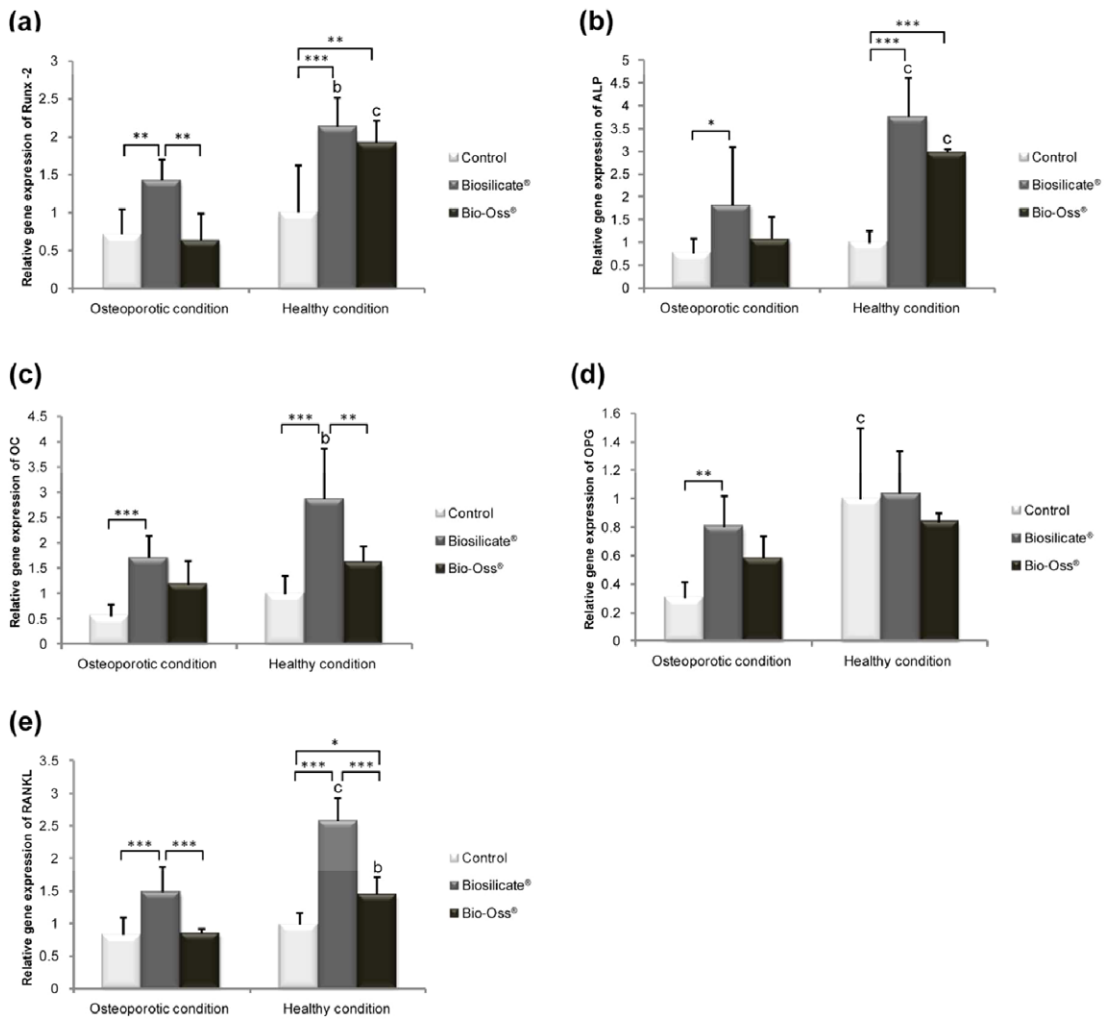

Figure 7. (a)–(e) *In vivo* results (mean ±SD) of the relative quantification of gene expression in osteoporotic ($n \geq 6$) and healthy conditions ($n \geq 5$). (a) Runx-2 gene-expression. (b) ALP gene-expression. (c) OC gene-expression. (d) OPG gene-expression. (e) RANKL gene-expression; * $p < 0.05$, ** $p < 0.01$ and *** $p < 0.001$, (b) $p < 0.01$ and (c) $p < 0.001$ compared to osteoporotic condition of same material.

more about the long term results, a second and later time point is needed.

Bioactive glasses and glass-ceramics, including Biosilicate®, belong to the third generation of biomaterials that are able to stimulate bone regeneration by cell response at a molecular level [29, 33, 47]. Our study confirms the positive effect of Biosilicate® at a molecular level by an increased relative expression of Runx-2, ALP, OPG, OC and RANKL. However, by histomorphometry bone formation was not increased significantly compared to Bio-Oss®. These results are in line with the study of Välimäki *et al* [48], who found that bioactive glass-ceramics not only promote osteoblastic functions, but also osteoclastic bone resorption and thereby enhancing bone turnover. Our study showed a significant up-regulation of osteoclastic RANKL expression by Biosilicate®, leading to a stimulation of osteoblasts enhancing bone turnover. The exact underlying mechanism of this effect remains unclear, but an enhanced bone turnover could explain why up-regulated osteogenic gene-expression does not lead to more bone formation. An additional explanation for the discrepancy between gene-expression and histomorphometric quantification is related to the osteoconductive capacity of both Biosilicate® and Bio-Oss®. The bone formation toward the centre of the defect is guided over the surface of the particulate materials, which likely masks the osteopromotive effects of Biosilicate®.

5. Conclusions

The present study comparatively evaluated the performance of two commercially available bone substitutes, Biosilicate® and Bio-Oss®, by measuring *in vitro* biological responses and *in vivo* experiments with rats in osteoporotic and healthy bone conditions. The main *in vitro* findings showed that Biosilicate® had a favourable osteopromotive effect on rat bone marrow-derived mesenchymal stem cells compared to Bio-Oss®.

While for the healthy condition, both Biosilicate® and Bio-Oss® did not improve bone formation, the *in vivo* performance of both materials showed improved bone regeneration in osteoporotic bone condition, particularly for Bio-Oss®. Gene-expression analysis *in vivo*

showed that Biosilicate® increases the expression for both osteoblast and osteoclast regulating genes, while Bio-Oss® only increases expression of genes for osteoblast differentiation. Since both materials improved bone regeneration in osteoporotic conditions, these data suggest that bone defects in osteoporotic conditions can be efficiently treated with synthetic bone substitutes.

Acknowledgments

The authors thank CAPES (Coordenação de Aperfeiçoamento de Pessoal de Nível Superior) for financial support. Author 1 and Author 2 contributed equally to this work. EDZ, OP and MCC are thankful to CNPq and the São Paulo funding agency Fapesp—grant # 2013/07793-6.

References

[1] Urist M R, Mazet R Jr and Mc L F 1954 The pathogenesis and treatment of delayed union and non-union; a survey of eighty-five ununited fractures of the shaft of the tibia and one hundred control cases with similar injuries *J. Bone Joint Surg. Am.* **36-A** 931–80

[2] Giannoudis P V, Einhorn T A and Marsh D 2007 Fracture healing: the diamond concept *Injury* **38** (Suppl. 4) S3–6

[3] Van der Stok J, Van Lieshout E M, El-Massoudi Y, Van Kralingen G H and Patka P 2011 Bone substitutes in the Netherlands—a systematic literature review *Acta Biomater.* **7** 739–50

[4] Dimitriou R, Mataliotakis G I, Angoules A G, Kanakaris N K and Giannoudis P V 2011 Complications following autologous bone graft harvesting from the iliac crest and using the RIA: a systematic review *Injury* **42** (Suppl. 2) S3–15

[5] Goulet J A, Senunas L E, DeSilva G L and Greenfield M L 1997 Autogenous iliac crest bone graft. Complications and functional assessment *Clin. Orthop. Relat. Res.* **339** 76–81

[6] Bongio M, Van den Beucken J J J P, Leeuwenburgh S C G and Jansen J A 2010 Development of bone substitute materials: from 'biocompatible' to 'instructive' *J. Mater. Chem.* **20** 8747–59

[7] Kurien T, Pearson R G and Scammell B E 2013 Bone graft substitutes currently available in orthopaedic practice: the evidence for their use *Bone Joint J.* **95-B** 583–97

[8] Carmona R H, Beato C, Lawrence A, Moritsugu K, Noonan A S and Katz S I 2004 1.1. A public health approach to promote bone health—the challenge *Bone Health and Osteoporosis: a Report of the Surgeon General* ed J A McGowan *et al* (Rockville MD: Office of the Surgeon General US)

[9] Johnell O and Kanis J A 2006 An estimate of the worldwide prevalence and disability associated with osteoporotic fractures *Osteoporos. Int.* **17** 1726–33

[10] Burge R, Dawson-Hughes B, Solomon D H, Wong J B, King A and Tosteson A 2007 Incidence and economic burden of osteoporosis-related fractures in the United States 2005–2025 *J. Bone Miner. Res.* **22** 465–75

[11] Baran D T 2000 Osteoporosis: which current treatments reduce fracture risk? *Cleve. Clin. J. Med.* **67** 701–3

[12] Meyer D, Stavropolous S, Diamond B, Shane E and Green P H 2001 Osteoporosis in a north american adult population with celiac disease *Am. J. Gastroenterol.* **96** 112–9

[13] Xiao Y, Fu H, Prasadam I, Yang Y C and Hollinger J O 2007 Gene expression profiling of bone marrow stromal cells from juvenile, adult, aged and osteoporotic rats: with an emphasis on osteoporosis *Bone* **40** 700–15

[14] Kubo T, Shiga T, Hashimoto J, Yoshioka M, Honjo H, Urabe M, Kitajima I, Semba I and Hirasawa Y 1999 Osteoporosis influences the late period of fracture healing in a rat model prepared by ovariectomy and low calcium diet *J. Steroid Biochem.* **68** 197–202

[15] Hollinger J O, Onikepe A O, MacKrell J, Einhorn T, Bradica G, Lynch S and Hart C E 2008 Accelerated fracture healing in the geriatric, osteoporotic rat with recombinant human platelet-derived growth factor-BB and an injectable beta-tricalcium phosphate/collagen matrix *J. Orthop. Res.* **26** 83–90

[16] Clupper D C, Gough J E, Hall M M, Clare A G, LaCourse W C and Hench L L 2003 *In vitro* bioactivity of S520 glass fibers and initial assessment of osteoblast attachment *J. Biomed. Mater. Res.* A **67** 285–94

[17] Thomas M V, Puleo D A and Al-Sabbagh M 2005 Bioactive glass three decades on *J. Long Term Eff. Med. Implants* **15** 585–97

[18] Greenwald A S, Boden S D, Goldberg V M, Khan Y, Laurencin C T and Rosier R N 2001 Bone-graft substitutes: facts, fictions, and applications *J. Bone Joint Surg. Am.* **83-A** (Suppl. 2 Part 2) 98–103

[19] Tapety F I, Amizuka N, Uoshima K, Nomura S and Maeda T 2004 A histological evaluation of the involvement of Bio-Oss in osteoblastic differentiation and matrix synthesis *Clin. Oral Implants Res.* **15** 315–24

[20] Orsini G, Scarano A, Degidi M, Caputi S, Iezzi G and Piattelli A 2007 Histological and ultrastructural evaluation of bone around Bio-Oss particles in sinus augmentation *Oral Dis.* **13** 586–93

[21] Abushahba F, Renvert S, Polyzois I and Claffey N 2008 Effect of grafting materials on osseointegration of dental implants surrounded by circumferential bone defects. An experimental study in the dog *Clin. Oral Implants Res.* **19** 329–34

[22] Orsini G, Traini T, Scarano A, Degidi M, Perrotti V, Piccirilli M and Piattelli A 2005 Maxillary sinus augmentation with Bio-Oss particles: a light, scanning, and transmission electron microscopy study in man *J. Biomed. Mater. Res. B Appl. Biomater.* **74** 448–57

[23] Lu H H, Tang A, Oh S C, Spalazzi J P and Dionisio K 2005 Compositional effects on the formation of a calcium phosphate layer and the response of osteoblast-like cells on polymer-bioactive glass composites *Biomaterials* **26** 6323–34

[24] Maquet V, Boccaccini A R, Pravata L, Notingher I and Jerome R 2003 Preparation, characterization, and *in vitro* degradation of bioresorbable and bioactive composites based on Bioglass-filled polylactide foams *J. Biomed. Mater. Res.* A **66** 335–46

[25] Freeman C O, Brook I M, Johnson A, Hatton P V, Hill R G and Stanton K T 2003 Crystallization modifies osteoconductivity in an apatite-mullite glass-ceramic *J. Mater. Sci. Mater. Med.* **14** 985–90

[26] Peitl O, Zanotto E D, Serbena F C and Hench L L 2012 Compositional and microstructural design of highly bioactive P_2O_5-Na_2O-CaO-SiO_2 glass-ceramics *Acta Biomater.* **8** 321–32

[27] Vogel M, Voigt C, Knabe C, Radlanski R J, Gross U M and Muller-Mai C M 2004 Development of multinuclear giant cells during the degradation of Bioglass particles in rabbits *J. Biomed. Mater. Res.* A **70** 370–9

[28] Hench L L 2006 The story of Bioglass *J. Mater. Sci. Mater. Med.* **17** 967–78

[29] Hench L L and Polak J M 2002 Third-generation biomedical materials *Science* **295** 1014–7

[30] Granito R N *et al* 2011 *In vivo* biological performance of a novel highly bioactive glass-ceramic (Biosilicate(R)): a biomechanical and histomorphometric study in rat tibial defects *J. Biomed. Mater. Res. B Appl. Biomater.* **97** 139–47

[31] Granito R N, Ribeiro D A, Renno A C, Ravagnani C, Bossini P S, Peitl-Filho O, Zanotto E D, Parizotto N A and Oishi J 2009 Effects of biosilicate and bioglass 45S5 on tibial bone consolidation on rats: a biomechanical and a histological study *J. Mater. Sci. Mater. Med.* **20** 2521–6

[32] Bossini P S, Renno A C, Ribeiro D A, Fangel R, Peitl O, Zanotto E D and Parizotto N A 2011 Biosilicate(R) and low-level laser therapy improve bone repair in osteoporotic rats *J. Tissue Eng. Regen. Med.* **5** 229–37

[33] Xynos I D, Edgar A J, Buttery L D, Hench L L and Polak J M 2001 Gene-expression profiling of human osteoblasts

following treatment with the ionic products of Bioglass 45S5 dissolution *J. Biomed. Mater. Res.* **55** 151–7
[34] Alghamdi H S, van den Beucken J J and Jansen J A 2014 Osteoporotic rat models for evaluation of osseointegration of bone implants *Tissue Eng. C Methods* **20** 493–505
[35] Zanotto E D, Ravagnani C, Peitl O, Panzeri H and Lara E H G 2004 Process and compositions for preparing particulate, bioactive or resorbable biosilicates for use in the treatment of oral ailments *Patent Application No. Int. C. C03C10/00, WO 2004/074199*
[36] Wallace K E, Hill R G, Pembroke J T, Brown C J and Hatton P V 1999 Influence of sodium oxide content on bioactive glass properties *J. Mater. Sci. Mater. Med.* **10** 697–701
[37] Ozawa S and Kasugai S 1996 Evaluation of implant materials (hydroxyapatite, glass-ceramics, titanium) in rat bone marrow stromal cell culture *Biomaterials* **17** 23–9
[38] Renno A C, McDonnell P A, Crovace M C, Zanotto E D and Laakso L 2010 Effect of 830 nm laser phototherapy on osteoblasts grown *in vitro* on Biosilicate scaffolds *Photomed. Laser Surg.* **28** 131–3
[39] Herten M, Rothamel D, Schwarz F, Friesen K, Koegler G and Becker J 2009 Surface- and nonsurface-dependent *in vitro* effects of bone substitutes on cell viability *Clin. Oral Investig.* **13** 149–55
[40] Sollazzo V, Palmieri A, Scapoli L, Martinelli M, Girardi A, Alviano F, Pellati A, Perrotti V and Carinci F 2010 Bio-Oss(R) acts on stem cells derived from peripheral blood *Oman Med. J.* **25** 26–31
[41] Jee W S and Yao W 2001 Overview: animal models of osteopenia and osteoporosis *J. Musculoskelet. Neuronal Interact.* **1** 193–207
[42] Turner R T, Maran A, Lotinun S, Hefferan T, Evans G L, Zhang M and Sibonga J D 2001 Animal models for osteoporosis *Rev. Endocr. Metab. Disord.* **2** 117–27
[43] Thompson D D, Simmons H A, Pirie C M and Ke H Z 1995 FDA Guidelines and animal models for osteoporosis *Bone* **17** 125S–33
[44] Francisco J I, Yu Y, Oliver R A and Walsh W R 2011 Relationship between age, skeletal site, and time post-ovariectomy on bone mineral and trabecular microarchitecture in rats *J. Orthop. Res.* **29** 189–96
[45] El Khassawna T *et al* 2013 Effects of multi-deficiencies-diet on bone parameters of peripheral bone in ovariectomized mature rat *PloS One* **8** e71665
[46] Rissanen J P, Suominen M I, Peng Z and Halleen J M 2008 Secreted tartrate-resistant acid phosphatase 5b is a Marker of osteoclast number in human osteoclast cultures and the rat ovariectomy model *Calcif. Tissue Int.* **82** 108–15
[47] Jones J R 2013 Review of bioactive glass: from hench to hybrids *Acta Biomater.* **9** 4457–86
[48] Valimaki V V, Yrjans J J, Vuorio E I and Aro H T 2005 Molecular biological evaluation of bioactive glass microspheres and adjunct bone morphogenetic protein 2 gene transfer in the enhancement of new bone formation *Tissue Eng.* **11** 387–94
[49] Chaves M D, De Souza Nunes L S, De Oliveira R V, Holgado L A, Filho H N, Matsumoto M A and Ribeiro D A 2012 Bovine hydroxyapatite (Bio-Oss((R))) induces osteocalcin, RANK-L and osteoprotegerin expression in sinus lift of rabbits *J. Craniomaxillofac. Surg.* **40** e315–20
[50] Wong R W and Rabie A B 2010 Effect of bio-oss collagen and collagen matrix on bone formation *Open Biomed Eng. J.* **4** 71–6
[51] Desterro Fde P, Sader M S, Soares G D and Vidigal G M Jr 2014 Can inorganic bovine bone grafts present distinct properties? *Braz. Dent. J.* **25** 282–8
[52] Van de Watering F C, Laverman P, Cuijpers V M, Gotthardt M, Bronkhorst E M, Boerman O C, Jansen J A and Van den Beucken J J J P 2013 The biological performance of injectable calcium phosphate/PLGA cement in osteoporotic rats *Biomed. Mater.* **8** 035012